KSCE Journal of Civil Engineering (2015) 19(4):1174-1182

DOI 10.1007/s12205-013-0749-3

Water Engineering

pISSN 1226-7988, eISSN 1976-3808
www.springer.com/12205

Discharge Coefficient and Energy Dissipation over Stepped Spillway under Skimming Flow Regime

Hossein Shahheydari*, Ehsan Jafari Nodoshan, Reza Barati***, and Mehdi Azhdary Moghadam******

Received December 22, 2013/Revised March 27, 2014/Accepted May 10, 2014/Published Online November 21, 2014

Abstract

Stepped spillways have a wide range of applicability as a hydraulic structure in large dams to dissipate energy of high-velocity flows at a downstream area of dams as well as release overflows into the downstream. In this study, the numerical simulation of the flow over the stepped spillway was investigated by using Flow3D software as an analytic flow field. The RNG k-ε model was applied as the turbulence model, and Volume of Fluid (VOF) model was used to determine the free surface flow profiles. At the first stage, the model was verified by reliable experimental data. Then, in order to investigate the various features of skimming flow regime, 112 numerical spillway models was designed, which 96 models were stepped spillway models and 16 models were smooth spillway models (i.e., WES profile). In these numerical experiment, two step sizes, six configuration, four passing discharge and four profile slopes (15, 30, 45 and 60 degrees) with various relative discharges were considered to investigate the energy dissipation and discharge coefficient rates. The results indicated that discharge coefficient rate and energy dissipation rate have inverse relationship. Also it was observed that when relative discharges increased, energy dissipation rate decreased and discharge coefficient rate increased.

Keywords: *stepped spillway, discharge coefficient, energy dissipation, Flow3D software*

1. Introduction

A spillway is usually one of the most important appurtenant facility of a dam. The act of a spillway is to provide an efficient and safe means of conveying flood discharges to the downstream area of dams (Azhdary Moghaddam, 1997). Improperly designed spillways or insufficient capacity of spillways can cause failures of dams (Frizell, 1991). Several factors such as the design flood, size and operation of the reservoir, and type and location of the dam are primarily important in the spillway design procedure.

The spillway's outlet structure must be designed to ensure that the spillway discharges will not erode the downstream channel bed, or undermine the toe of the dam itself because the flow accelerates along the downstream face and high velocities (i.e., Froude numbers greater than 2.5) are attained at the spillway's toe. Traditionally, the energy dissipators for spillways can be classified as (Khatsuria, 2004): (1) Stilling basins, (2) free jets and trajectory buckets, (3) roller buckets, (4) dissipation by spatial hydraulic jump, and (5) impact type energy dissipators. However, it should be noted that stilling basin of multi-horizontal submerged jets (Chen *et al*., 2010; 2013; 2014; Zhang *et al*., 2013) and vortex drop shaft with two aeration volute chambers (Zhao *et al*., 2006; Gang *et al*., 2011) are available as new types of energy dissipators. Several factors such as hydraulic and environmental conditions, geology, topography, dam type and economic considerations are important for the selection of the type of the energy dissipator. The use of the stilling basin is the most common type of the energy dissipator. The traditional stilling basins are not suggested for heads exceeding about 100 m because the turbulence problems such as intermittent cavitation, vibration, uplift, and hydrodynamic loading appears in these conditions (Khatsuria, 2004). However, the energy dissipator of stilling basin of multi-horizontal submerged jets was used in a hydraulic engineering with the water head about 161 m (Chen *et al*., 2010; 2013; 2014; Zhang *et al*., 2013). Generally, the development of the stilling basin in hydraulic engineering is based on the form of the hydraulic jump, which depend on the expected Froude number of the incoming flow. The form of the stilling basin can range from a simple concrete apron to a complex structure that may include rows of chute blocks, baffle piers and a plain or dentate end sill (Peterka, 1958; USBR, 1977). For more details, the reader is referred to USBR

*P.G. Researcher, University of Sistan and Baluchestan, Zahedan 98155-987, Iran (E-mail: a_shahheydari@yahoo.com)
**Ph.D. Candidate, Semnan University, Semnan 19111-35131, Iran (E-mail: Ehsan_jafari64@yahoo.com)
***Ph.D. Candidate, Tarbiat Modares University, Tehran 14115-143, Iran (Corresponding Author, E-mail: r88barati@gmail.com)
****Associate Professor, University of Sistan and Baluchestan, Zahedan 98155-987, Iran (E-mail: mazhdary@eng.usb.ac.ir)

(1977) and Khatsuria (2004). The length of the stilling basin located at the foot of the spillway should be kept as short as possible. In order to reach this goal, one possible solution is to consider a stepped spillway instead of the traditional smooth ogee-profile spillway. Stepped chutes which is a spillway whose face is provided with a series of steps from near the crest to the toe, have become a standard hydraulic structure within the past decades (Vischer and Hager, 1998). The steps significantly increase the rate of energy dissipation taking place on the spillway face. Therefore, they can reduce the size of the required downstream energy dissipation basin.

On the other hand, the use of a stepped spillway can reduce the risk of cavitation than more conventional smooth spillways by increasing self-aerated flow (Peterka, 1953; Frizell and Melford, 1991; Boes and Hager, 2003; Lobosco, 2011; Felder and Chanson, 2014b). It should be stated that no evidence of the cavitation damage has been seen for a stepped spillway in service because of relatively steep slopes. According to cavitation indications, the use of stepped spillways with relatively steep slopes will be less susceptible to cavitation damage (Frizell *et al*., 2013). However, there has been significant uncertainty in how to address cavitation on stepped spillways (Arndt and Ippen, 1968; Boes and Hager, 2003; Pfister *et al*., 2006; Gomes *et al*., 2007; Amador *et al*., 2009; Frizell *et al*., 2013; Khdhiri *et al*., 2014).

The priority of the stepped spillways is not limited to the aforementioned topics. This type of spillway may be designed in several forms such as nonuniform steps, downward inclined steps, changing channel slope and pooled step (Felder and Chanson, 2014b). Moreover, stepped spillways are compatible with Roller Compacted Concrete (RCC) as a modern construction technique and with gabion hydraulic structures as a common retaining structure. Also, in the case of an auxiliary spillway the construction program will be much shortened.

From the foregoing reasons, and also low cost of stepped spillways, there are a most of interest in this form of spillway (e.g. Sorensen, 1985; Frizell, 1991; Chanson, 2002; Chanson and Toombes, 2002; Baylar *et al*., 2007; Baylar *et al*., 2010; Emiroglu and Tuna, 2011; Baylar *et al*., 2011a, 2011b; Meireles *et al*., 2012; Frizell *et al*., 2012; Dolatshah and Vosoughifar, 2012; Zhang *et al*., 2012; WU *et al*., 2013; Roushangar *et al*., 2014; Felder and Chanson, 2014b). The flow characteristics over stepped chute were investigated numerically and experimentally in these studies. Most of them have been focused on the inception of air entrainment, air concentration, velocity distributions, and energy dissipation performance of a stepped chute.

Parenthetically, it should be noted that three types of flow regimes (i.e., nappe, transition and skimming flow) are possible over a stepped spillway (Essery and Horner, 1978; Sorensen, 1985; Chanson, 1998; Khdhiri *et al*., 2014). The first flow, which is a series of small consecutive falls, occurs for low water flowrates and/or important steps lengths, whereas the latter, which consists of recirculation zones with horizontals axes between steps outer edges, arises for high flowrates and/or small steps lengths. Finally, the transition flow regime, which was firstly introduced by Ohtsu and Yasuda (1997), appears for passing from nappe flow regime to skimming flow regime for a range of intermediate discharges. The main characteristic of this regime is that the stagnation on the horizontal step face associated with significant splashing appears.

Since physical measurements are expensive and time consuming, computational modeling is an effective and convenient approach (Barati, 2011; Akbari and Barati, 2012; Barati *et al*., 2012; 2013; Barati, 2013). Therefore, the numerical simulation of flow over stepped spillways would be in a great demand. In the present study, the computational fluid dynamics model of FLOW3D software was adopted to simulate the flow over the stepped spillway under skimming flow regime. Volume of Fluid (VOF) method was performed for free surface simulation. Several factors consist of the step size and configuration, spillways slope and passing discharge were considered in the numerical experiments. The main objectives of this study are: (1) Investigation of the effects of step's configuration on discharge coefficient and energy dissipation; (2) Comparison between energy dissipation rate and discharge coefficient rate; (3) Study of effect of relative discharges on discharge coefficient and energy dissipation; (4) Analysis of effect of spillway's slope on energy dissipation and discharge coefficient rate; and (5) Find an optimum step's configuration to reach the maximum energy dissipation and maximum passing flow.

2. Governing Equation and General Issues

2.1 Problem Formulation

FLOW-3D software which is a general purpose CFD software for modeling multi-physics flow problems was adopted for the simulation of the flow over stepped spillway.

The software utilizes a Hirt-Nichols' VOF method to compute free surface motion. It uses an approximate interface reform that is parallel to one of the co-ordinate axes. While cells in a neighborhood are utilized to estimate the surface normal, the interface is marked as horizontal or vertical depending on the relative magnitudes of the surface normal components (Rudman, 1997). The VOF method not only introduces a VOF function, $F(x, y, z, t)$, but also consists of the following three ingredients: (1) a scheme to locate the surface; (2) an algorithm to track the surface as a sharp interface moving through a computational grid; and (3) a means of applying boundary conditions at the surface. The Fractional Area/Volume Obstacle Representation technique was used to model complex geometric regions.

FLOW-3D uses a finite-volume-finite difference method to discretize the 3D Reynolds-averaged Navier-Stokes equations in a fixed Eulerian rectangular grid system. For each computational cell, average values for the flow variable (i.e., pressure and velocity field) are computed at discrete times using a staggered grid technique. The governing equations can be expressed as (Savage and Johnson, 2001):

Continuity equation:

$$\frac{\partial}{\partial x}(uA_x)+R\frac{\partial}{\partial_y}(vA_y)+\frac{\partial}{\partial_z}(wA_z)+\xi\frac{uA_x}{x}=\frac{RSOR}{\rho} \tag{1}$$

where, ρ is the density of fluid, RSOR is the mass source, u, v, w respectively are velocity in x, y, z directions in Cartesian coordinate, and A_x, A_y, A_z are differential area in these directions. R and ξ depends on coordinate system and in Cartesian coordinate R = 1 and ξ = 0.

Momentum equations:

$$\frac{\partial_u}{\partial_t}+\frac{1}{V_F}\left\{uA_x\frac{\partial_u}{\partial_x}+vA_yR\frac{\partial_u}{\partial_y}+wA_z\frac{\partial_u}{\partial_z}\right\}-\xi\frac{A_yv^2}{xV_F}= -\frac{1}{\rho}\frac{\partial_p}{\partial_x}+G_x+f_x-b_x-\frac{RSOR}{\rho V_F}u \tag{2}$$

$$\frac{\partial_v}{\partial_t}+\frac{1}{V_F}\left\{uA_x\frac{\partial_v}{\partial_x}+vA_yR\frac{\partial_v}{\partial_y}+wA_z\frac{\partial_v}{\partial_z}\right\}+\xi\frac{A_yuv}{xV_F}= -\frac{1}{\rho}R\frac{\partial_p}{\partial_y}+G_y+f_y-b_y-\frac{RSOR}{\rho V_F}v \tag{3}$$

$$\frac{\partial_w}{\partial_t}+\frac{1}{V_F}\left\{uA_x\frac{\partial_w}{\partial_x}+vA_yR\frac{\partial_w}{\partial_y}+wA_z\frac{\partial_w}{\partial_z}\right\}= -\frac{1}{\rho}\frac{\partial_p}{\partial_{zx}}+G_z+f_z-b_z-\frac{RSOR}{\rho V_F}w \tag{4}$$

where, V_F is the fraction of fluid, G_x, G_y, G_z are body acceleration, f_x, f_y, f_z are acceleration due to viscosity and b_x, b_y, b_z are flow losses in porous media.

Several turbulence closure are available in FLOW-3D. Renormalized-group turbulence model (RNG) which is generally the most robust transport turbulence model available within the software was adopted for the simulation of the turbulent flow over the stepped spillway (Yakhot and Smith, 1992; Yakhot *et al.*, 1992; Flow Science Inc., 2005). The eddy viscosity is calculated using a single turbulence length scale in the standard k-ε model. Therefore, the turbulent diffusion is only determined at the specified scale, whereas all turbulence scales will contribute to the turbulent diffusion in reality. RNG k-ε model accrues from the renormalization group mathematical theory. An extra source term to the turbulence kinetic energy dissipation ε transport equation was added in RNG model to improve standard k-ε model in determining the turbulence kinetic energy. Also, some constants of RNG k-ε model is different than k-ε model's coefficients.

The governing equations of RNG k-ε model (i.e., k and ε transport equations, respectively) are:

$$\frac{\partial k}{\partial t}+u_j\frac{\partial k}{\partial x_j}=\frac{\partial}{\partial x_j}\left[\left(v+\frac{v_t}{\sigma_k}\right)\frac{\partial k}{\partial x_j}\right]+G-\varepsilon \tag{5}$$

$$\frac{\partial \varepsilon}{\partial t}+u_j\frac{\partial \varepsilon}{\partial x_j}=\frac{\partial}{\partial x_j}\left[\left(v+\frac{v_t}{\sigma_\varepsilon}\right)\frac{\partial \varepsilon}{\partial x_j}\right]+C_{\varepsilon 1}\frac{\varepsilon}{k}G-C_{\varepsilon_2}\frac{\varepsilon^2}{k}-C_\mu\eta^3\frac{1-\eta/\eta_0}{1+\beta\eta^3}\frac{\varepsilon^2}{k} \tag{6}$$

Table 1. Constants of RNG k-ε Model

β	η_0	C_μ	$C_{\varepsilon 1}$	$C_{\varepsilon 2}$	σ_k	σ_ε
0.012	4.38	0.085	1.42	1.68	0.7194	0.7194

where, k is the turbulence kinetic energy, ε is dissipation rate, $v_t = C_\mu k^2/\varepsilon$ is the eddy viscosity, v is the kinematic viscosity, and other parameters defined as:

$$G=v_t\left(\frac{\partial u_i}{\partial x_j}+\frac{\partial u_j}{\partial x_i}\right)\frac{\partial u_i}{\partial x_j} \tag{7}$$

$$\eta=\frac{k}{\varepsilon}\left(\frac{G}{v_t}\right)^{0.5} \tag{8}$$

The constants of RNG k-ε model were listed in Table 1.

2.2 Numerical Simulation Issues

Some issues of the numerical simulation such as the mesh independency investigation, boundary conditions, air entrainment coefficient, uniform flow conditions, and time step will be discussed in this section.

The computational domain mesh was adopted using mesh independency study (i.e., grid convergence tests) using the experimental data of Azhdary Moghaddam (1995) (see more details about the experiments in the verification section**)**. Over 100 numerical tests from 30,000 to 811,200 computational cells were performed to reach the proper mesh. The selected mesh consists of a total of 625,000 computational cells in the simulation domain (250 × 250 × 10 in x, z and y directions which represent stream-wise, normal-wise and span-wise coordinates, respectively). The mesh grid was composed using three different mesh blocks, and finer mesh was used near the spillway (see Fig. 1). It should be noted that the numbers of computational cells in x and z directions have more effects on the simulation results.

Four types of boundary conditions for inlet, outlet, wall and free surface were adopted. A specified pressure boundary condition (i.e., a stagnation pressure condition) was used at the upstream end of the computational region (i.e., x_{min}). In this boundary condition, the velocity at the boundary is zero because stagnation conditions is assumed in the outside of the boundary. This assumption needs a pressure drop across the boundary for flow to enter the computational region (Flow Science, 2005). Continuative approximation which consist of zero normal

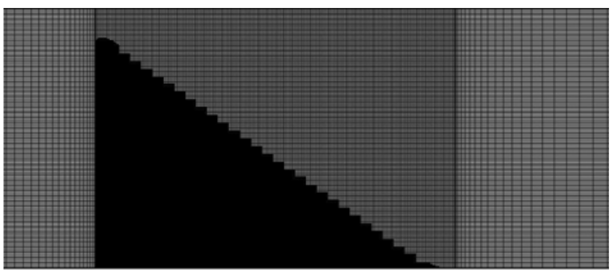

Fig. 1. Mesh Grid Configuration for the Numerical Simulation

derivatives at the boundary for all quantities was considered at the downstream end of the computational region (i.e., x_{max}). In this boundary condition, a smooth continuation of the flow through the boundary was represented by the zero-derivative condition. In left, right and bottom sides of the computational region (i.e., y_{min}, y_{max} and z_{min}, respectively), the normal velocity is set to zero by considering a wall boundary condition. Finally, normal velocity as well as normal gradients of all variables is set to zero (i.e., symmetry boundary condition) at z_{max}.

Oxygen transfer in stepped spillways depends on several factors such as the step height, flow critical height, steps length, stepped spillway total height, inflow Reynolds number, and global spillway slope (Khdhiri *et al*., 2014). All of these factors effects on the turbulence that increase air entrainment in water at interface between air and water. In contrast to transition flows, the air concentration profiles have a smooth and continuous shape in skimming flows (Chanson and Toombes, 2002; Chanson, 2002). In the skimming flow regime, the flow is smooth and no air entrainment occurs in the upstream steps while a large amount of flow aeration and strong vortices at the step toes arises in the downstream of the flow. Based on previous studies, average concentrations of air (i.e., air entrainment coefficient) for skimming flow was considered 20%. This average value can be assigned in the physics menu at air entrainment section of FLOW-3D software.

The length of upstream water pool was considered 25 m, and 60 m was assigned after the toe of the dam to reach the developed flow and uniform flow conditions at the downstream section. It could be stated that FLOW-3D software alert the user in the simulate menu when the developed flow condition was obtained. Also, it should be noted that the simulation time for reaching uniform flow conditions increased by increasing discharge.

Finally, it must be stated that the time step was considered based on the stability limit and convergence criteria by a trial and error procedure. The time step increment was performed in the range of 0.00001-0.01 (s), and the proper value 0.001 (s) was considered en-route to convergence.

3. Results and Discussion

3.1. Verification using Experimental Data

In order to evaluate the applicability and accuracy of the model, Experimental data of Azhdary Moghaddam (1995), which was performed in hydraulic Laboratory University of Ottawa, was considered. For the comparison propose, free surface level of model and experimental data was taken.

The spillway crest geometry of Waterways Experiment Station (1977) with vertical upstream faces was considered. It includes the three-arc curve upstream from the crest section. Downstream from the crest, the following power function applies as:

$$\left(\frac{y}{H_D}\right) = 0.5\left(\frac{x}{H_D}\right)^{1.85} \tag{9}$$

where, H_D is design head.

The downstream slope with 45° and height of 380 mm was examined. Discharges passing over spillway, 0.026(m^3/s) and 0.05(m^3/s) was verified.

The numerical and experimental results for the location of the free surface are shown in Fig. 2 for two discharges. As most important variables, the velocity at the toe *V*, the height of flow at

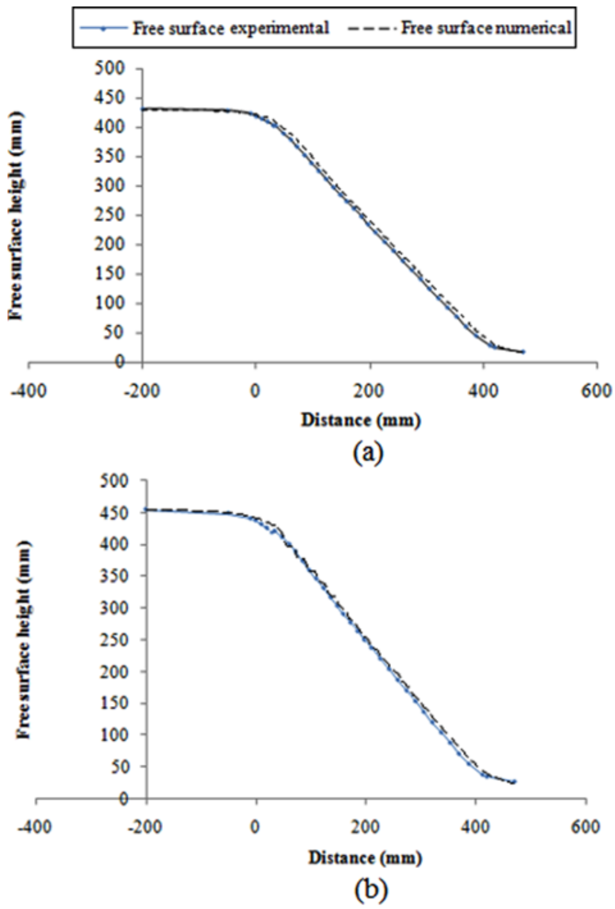

Fig. 2. Comparison between Free Surface Height for Numerical and Experimental Data: (a) Q = 0.026(m^3/s), (b) Q = 0.05(m^3/s)

Table 2. Verification of Model by Comparing Numerical Results and Experimental Data

	Q(m^3/s)	*V*(m/s)	*h*(m)	*Fr*	*E*(m)
Experiment results	0.026	1.440	0.0180	3.426	0.1236
	0.05	1.851	0.0270	3.596	0.2016
Numerical results	0.026	1.483	0.0184	3.490	0.1305
	0.05	1.984	0.0253	3.982	0.2250

the toe h, Froude number Fr and the energy of flow $E = h+V^2/2g$ at the toe of experimental and numerical were compared in Table 2. Generally, the results indicated that good agreement between the computed and measured profiles can be concluded at the crest and toe portions of the spillway surface for the two passing discharges.

3.2 Numerical Experiments

In this study, Ogee smooth spillways and Ogee stepped spillways was considered for the comparison purpose. All ogee-profile spillways considered in this study had vertical upstream faces. It should be noted that the spillway was put on zero point of horizontal axis. The crest geometry of spillway was considered *WES* profile with $H_D = 3.75$(m). It includes the three-arc curve upstream from the crest section. The height of spillways was 30(m). This shape continues down to the point where the slope of the curve meets the terminal spillway slope. Four different terminal slopes were investigated, namely: 15°, 30°, 45°, and 60° and a 10 m radius of curvature was chosen for the spillway toe transition curve for all models. This ensured a smooth transition of the flow from the spillway to the downstream channel.

Stepped spillway configurations were examined by considering different downstream slopes, different step sizes, several numbers of the steps, and different arrangement of the steps. Also, four passing discharge were considered.

In Table 3 different downstream slopes (l/p) were listed, where, l is length of spillways and p is height of spillways.

Each of the base stepped models constructed in three parts: (1) the crest part, which was 1/3 of the total spillway height (H_{dam}), (2) the middle part which was 1/3 of the total spillway height (H_{dam}) and bottom part which had a height = 1/3 H_{dam}. While each part of the models had a uniform step size throughout its profile, the step sizes of the base models were different from each other. Based on the literature review (Sorensen, 1985, Christodoulou, 1993, Bindo, 1993, Rice and Kadavy, 1996) two different step sizes were chosen: (1) 1/20 H_{dam} which considered as large-step sizes; and (2) 1/30H_{dam} which considered as small-step sizes. Six following configuration's code for stepped spillways were considered:

(1) LLL: This configuration means that large step in top, middle and bottom part,
(2) LLS: This configuration means that large step in top and middle part and small step in bottom part,
(3) LSS: This configuration means that large step in top part and small step in middle and bottom part,
(4) SLL: This configuration means that small step in top part and large step in middle and bottom part,
(5) SSL: This configuration means that small step in top and middle part and large step in bottom part, and
(6) SSS: This configuration means that small step in top, middle and bottom part.

Table 3. l/p for all Spillway's Slopes

	l(m)	p(m)	l/p
15°	114.7500	30	3.8225
30°	56.7780	30	1.8926
45°	37.0500	30	1.2350
60°	27.3325	30	0.9110

In order to find the relative energy dissipation rate, energy at the toe of the stepped spillway models were compared with the energy at the toe of the smooth models.

The four relative head passing over the spillways (1) $H/H_D = 0.7$, (2) $H/H_D = 1$, (3) $H/H_D = 1.5$, and (4) $H/H_D = 2$ were selected for investigation of the amount of energy dissipation rate and the discharge coefficient, where H is total head at upstream and H_D is design head.

The discharge coefficients for 96 stepped spillway models and 16 smooth spillway models were determined. For the mentioned relative head, discharge coefficient for stepped models (C_s) and smooth models (C) divided to each other (C_s/C) and define as discharge coefficient rate. Also the percent of step's influence on passing flow was analyzed by considering the following equations:

$$Q_{stepped} = C_s L H^{3/2} \tag{10}$$

$$Q_{smooth} = C L H^{3/2} \tag{11}$$

where, C_s is the discharge coefficient for the stepped spillways, C is the discharge coefficient for the smooth spillways, L is the width of spillway, and H is the total head at upstream.

Several criteria were existed to show the onset of skimming flow that is a function of the discharge, the step height and length (Chanson, 1994). Based on the experimental data, Essery and Horner (1978) and Peyras *et al.* (1991) presented Eq. (12) for the onset flow condition:

$$\frac{(y_c)_{Onset}}{h} = 1.01 - 0.37\left(\frac{h}{l}\right) \tag{12}$$

where, h is the step height, l is the step length and $(y_c)_{Onset}$ is the characteristic critical depth. It should be noted that skimming flow will occur when $y_c/h > (y_c)_{Onset}/h$.

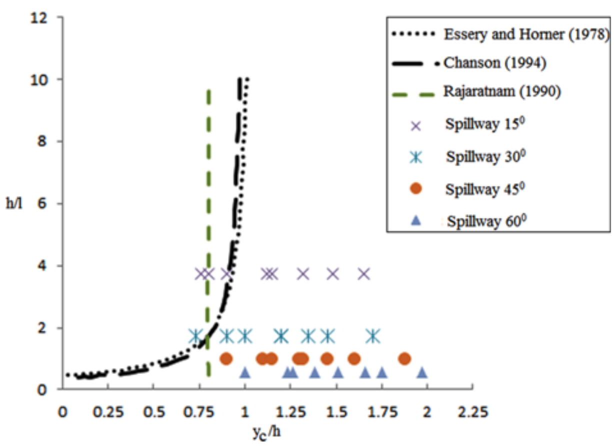

Fig. 3. Investigation of the Onset of Skimming Flow Regime

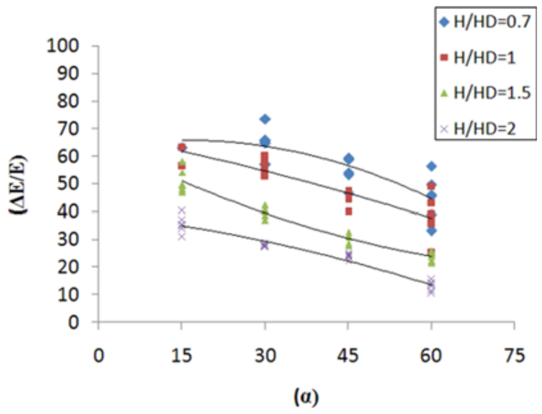

Fig. 4. Effect of Relative Head on Energy Dissipation

The criterion was revised by Chanson (1994) by re-analyzing experimental data as follows:

$$\frac{(y_c)_{Onset}}{h} = 1.057 - 0.456\left(\frac{h}{l}\right) \tag{13}$$

Moreover, Rajaratnam (1990) discussed that skimming flow will occur when $(y_c)_{Onset}/h$ > 0.8. All of the aforementioned criteria along with the numerical results for different spillway's slope are presented in Fig. 3. The results showed that skimming flow was not established in low discharges (H/H_D = 0.7, H/H_D = 1) and low spillway's slope; therefore, their data was removed from comparisons.

The results of the numerical analysis were illustrated in Figs. 4 to 7. In these figures, E and E are $E = h+V^2/2g$, $E = E_{smooth} - E_{stepped}$, where E is energy at the toe of the spillways; h is water surface height at the toe; and V is velocity of flow at the toe. It should be noted that the dimensionless energy (E/E) was calculated as $(E_{smooth} - E_{stepped})/ E_{smooth.}$

Figure 4 represents energy dissipation rate versus spillway's slopes (α) for different relative heads. As it can be seen in Fig. 4, the energy dissipation rate decreased with increasing relative head, and also it was observed that the energy dissipation rate increased by decreasing spillway's slopes. Therefore, for the design purpose, the use of stepped spillway with lower relative head and/or spillway's slopes can be considered to reach the maximum energy dissipation rate.

Figure 5 depicts energy dissipation rate versus spillway's slops for all configurations and relative discharges. In Fig. 5(a) and 5(b) (i.e. low discharges), one can find a rational configuration that was suitable energy dissipation rate. *SLL* configuration showed higher energy dissipation rate in Fig. 5(c) and 5(d) but effects of step's configuration was low in these relative discharges because of high discharges. At 60° downstream slope almost for all discharges, *LLL* configuration showed maximum energy dissipation. So, for the design purpose, it should be noticed that spillways with high downstream slopes and large steps can be applied.

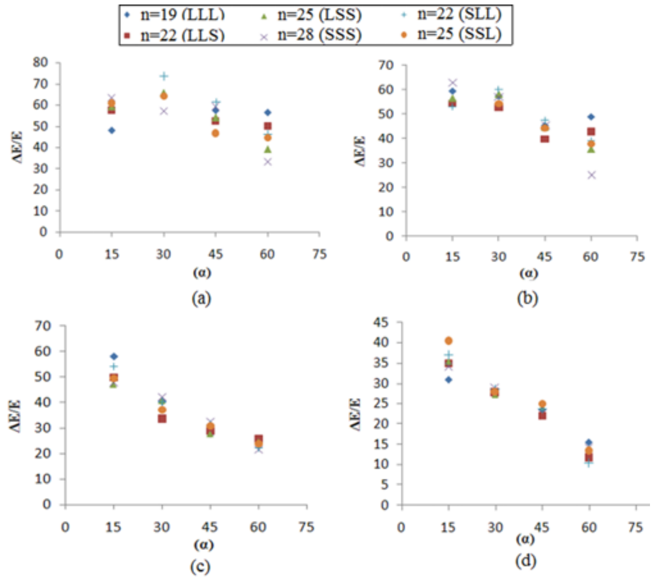

Fig. 5. Comparison between Energy Dissipation Rate and Spillway's Slope: (a) H/H_D = 0.7, (b) H/H_D = 1, (c) H/H_D = 1.5, (d) H/H_D = 2

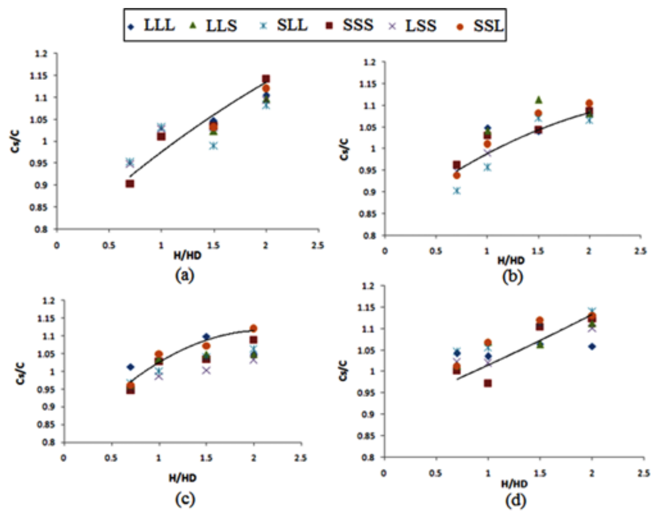

Fig. 6. Comparison of Ratio of Discharge Coefficients and Passing Discharge: (a) Spillway 15°, (b) Spillway 30°, (c) Spillway 45°, (d) Spillway 60°

Relationship between relative head and discharge coefficient rate for all step's configurations and downstream slops were presented in Fig. 6. The parameter C_s/C increased with increasing relative head, and also it was observed that discharge coefficient rate decreased by decreasing spillway's slopes. Therefore, for the design purpose, the use of stepped spillway with larger relative head and/or spillway's slopes can be assigned to reach the maximum discharge coefficient rate. On the other hand, it was observed that, among all configurations, *SSL* generally has maximum passing flow.

In Fig. 7, the relationship between energy dissipation rate and C_s/C parameter were illustrated. It was found that energy

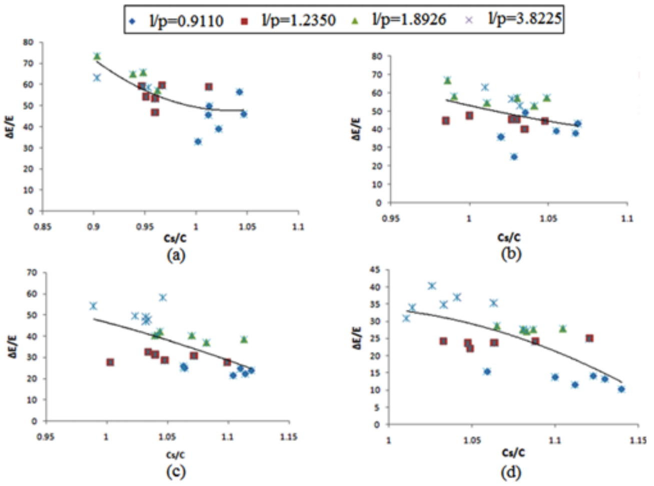

Fig. 7. Comparison of Percent of Energy Dissipation and Ratio of Discharge Coefficients: (a) H/H_D = 0.7, (b) H/H_D = 1, (c) H/H_D = 1.5, (d) H/H_D = 2

dissipation rate decreased with increasing slope of spillways, whereas C_s/C increased with increasing slope of spillways. These results are consistent with the previous results in Figs. 4 to 6.

Generally, it can be stated that with increasing relative head, energy dissipation rate decreased and discharge coefficient rate (C_s/C) increased. On the other hand, energy dissipation rate decreased and discharge coefficient rate increased with increasing slope of spillways. Therefore, an optimum relative head and spillway's slope must be assigned to reach the best possible energy dissipation rate and discharge coefficient.

On the other hand, for the optimal step configuration, it can be concluded that smaller steps at the crest part of the stepped spillway and larger steps at bottom part of the stepped spillway must be considered to reach both maximum energy dissipation and maximum passing flow.

4. Conclusions

Most of the previous studies of a stepped spillway have been only focused on the energy dissipation performance of it. However, in the present study, the discharge coefficient rate as well as the energy dissipation rate were considered for various flow conditions and several spillway layouts.

First of all, this study shows the priorities of an advanced CFD model, Flow3D, than expensive laboratory tests for the investigation of the flow over stepped spillways. At the first stage, in order to verify the numerical model, the water surface level of the model were compared with experimental free surface profiles. Then, the numerical experiments were designed to evaluate the effects of different factors on the skimming flow regime of stepped spillways. The stepped models were designed by considering two step size, six configuration, four different spillways slope below the contact point and four passing discharge in the numerical experiments.

Based on the results of the numerical experiments, the main conclusions of the present study are:

1. The discharge coefficient increased for the case of a stepped spillway in comparison with an equivalent smooth spillway. This issue provides more flood conveying capacity to the downstream channel in a given time period. On the other hand, it was previously proved that a stepped spillway increase energy dissipation rate than a smooth spillway.
2. To reach the maximum energy dissipation rate, the stepped spillway with lower relative head and/or spillway's slopes must be assigned in the design procedure of a stepped spillway, whereas to reach the maximum discharge coefficient rate, the stepped spillway with larger relative head and/or spillway's slopes can be considered in the design procedure of a stepped spillway. Therefore, an optimum relative head and spillway's slopes must be considered to reach the best possible energy dissipation rate and discharge coefficient.
3. Maximum energy dissipation and maximum passing flow were achieved when small and large steps respectively are considered at crest and bottom parts of the spillway. This issue can consider for the optimum design.

Acknowledgements

The writers thank the reviewers for their critical and constructive comments.

References

Akbari, G. H. and Barati, R. (2012). "Comprehensive analysis of flooding in unmanaged catchments." *Proceedings of the ICE-Water Management*, Vol. 165, No. 4, pp. 229-238, DOI: 10.1680/wama.10.00036.

Amador, A., Sánchez-Juny, M., and Dolz, J. (2009). "Developing flow region and pressure fluctuations on steeply sloping stepped spillways." *Journal of Hydraulic Engineering*, Vol. 135, No. 12, pp. 1092-1100, DOI: 10.1061/(ASCE)HY.1943-7900.0000118.

Arndt, R. E. and Ippen, A. T. (1968). "Rough surface effects on cavitation inception." *Journal of Basic Engineering*, Vol. 90, No. 2, pp. 249-261.

Azhdary Moghaddam, M. (1997). *The hydraulics of ogee-stepped spillway profile*, PhD Thesis, Ottawa, Canada.

Barati, R. (2011). "Parameter estimation of nonlinear Muskingum models using Nelder-Mead simplex algorithm." *Journal of Hydrologic Engineering*, Vol. 16, No. 11, pp. 946-954, DOI: 10.1061/(ASCE)HE.1943-5584.0000379.

Barati, R. (2013). "Application of excel solver for parameter estimation of the nonlinear Muskingum models." *KSCE Journal of Civil Engineering*, KSCE, Vol. 17, No. 5, pp. 1139-1148, DOI: 10.1007/s12205-013-0037-2.

Barati, R., Akbari, G., and Rahimi, S. (2013). "Flood routing of an unmanaged river basin using Muskingum-Cunge model; Field application and numerical experiments." *Caspian Journal of Applied Sciences Research*, Vol. 2, No. 6, pp. 08-20.

Barati, R., Rahimi, S., and Akbari, G. H. (2012). "Analysis of dynamic wave model for flood routing in natural rivers." *Water Science and Engineering*, Vol. 5, No. 3, pp. 243-258.

Baylar, A., Bagatur, T., and Emiroglu, M. E. (2007). "Aeration efficiency with nappe flow over stepped cascades." *Proceedings of the ICE-Water Management*, Vol. 160, No. 1, pp. 43-50, DOI: 10.1680/wama.2007.160.1.43.

Baylar, A., Unsal, M., and Ozkan, F. (2010). "Hydraulic structures in water aeration processes." *Water, Air, & Soil Pollution*, Vol. 210, No. 1-4, 87-100, DOI: 10.1007/s11270-009-0226-2.

Baylar, A., Unsal, M., and Ozkan, F. (2011a). "The effect of flow patterns and energy dissipation over stepped chutes on aeration efficiency." *KSCE Journal of Civil Engineering*, KSCE, Vol. 15, No. 8, pp. 1329-1334, DOI: 10.1007/s12205-011-1360-0.

Baylar, A., Unsal, M., and Ozkan, F. (2011b). "GEP modeling of oxygen transfer efficiency prediction in aeration cascades." *KSCE Journal of Civil Engineering*, KSCE, Vol. 15, No. 5, pp. 799-804, DOI: 10.1007/s12205-011-1282-x.

Bindo, M., Gautier, J., and Lacroix, F. (1993). "The stepped spillway of M'Bali Dam." *Int. Water Power & Dam Construction*, Vol. 45, No. 1, pp. 35-36.

Boes, R. and Hager, W. (2003). "Hydraulic design of stepped spillways." *Journal of Hydraulic Engineering*, Vol. 129, No. 9, pp. 671-679, DOI: 10.1061/(ASCE)0733-9429(2003)129:9(661).

Chanson, H. (1994). "Hydraulics of skimming flows over stepped channels and spillways." *Journal of Hydraulic Research*, Vol. 32, No. 3, pp. 445-460.

Chanson, H. (1998). "Review of studies on stepped channel flows." *Workshop on Flow Characteristics Around Hydraulic Structures and River Environment*, Nihon University, Tokyo, Japan (November).

Chanson, H. (2002). *The hydraulics of stepped chutes and spillways*, Balkema.

Chanson, H. and Toombes, L. (2002). *Air-water flows down stepped chutes: Turbulence and flow structure observations*, Department of Civil Engineering, University of Queensland, Brisbane, Australia.

Chen, J. G., Zhang, J. M., Xu, W. L., and Wang, Y. R. (2010). "Numerical simulation of the energy dissipation characteristics in stilling basin of multi-horizontal submerged jets." *Journal of Hydrodynamics*, Ser. B, Vol. 22, No. 5, pp. 732-741, DOI: 10.1016/S1001-6058(09)60110-4.

Chen, J. G., Zhang, J. M., Xu, W. L., Li, S., and He, X. L. (2013). "Particle image velocimetry measurements of vortex structures in stilling basin of multi-horizontal submerged jets." *Journal of Hydrodynamics*, Ser. B, Vol. 25, No. 4, pp. 556-563, DOI: 10.1016/S1001-6058(11)60396-0.

Chen, J., Zhang, J., Xu, W., and Peng, Y. (2014). "Characteristics of the velocity distribution in a hydraulic jump stilling basin with five parallel offset jets in a twin-layer configuration." *Journal of Hydraulic Engineering*, Vol. 140, No. 2, pp. 208-217, DOI: 10.1061/(ASCE)HY.1943-7900.0000817.

Christodoulou, G. C. (1993). "Energy dissipation on stepped spillway." *Journal of Hydraulic Engineering*, Vol. 119, No. 5, pp. 473-482, DOI: 10.1061/(ASCE)0733-9429(1993)119:5(644).

Dolatshah, A. and Vosoughifar, H. (2012). "Determination of aerated steps number over broad-crest stepped spillways under jet flow regime by using artificial neural network." *Journal of Water Sciences Research*, Vol. 4, No. 1, pp. 11-18.

Emiroglu, M. E. and Tuna, M.C. (2011). "The effect of tailwater depth on the local scour downstream of stepped-chutes." *KSCE Journal of Civil Engineering*, KSCE, Vol. 15, No. 5, pp. 907-915, DOI: 10.1007/s12205-011-0921-6.

Essery, I. T. S. and Horner, M. W. (1978). *The hydraulic design of stepped spillways*, Report 33 Constr. Industry Res. and Information Assoc., London, England.

Felder, S. and Chanson, H. (2014a). "Triple decomposition technique in air-water flows: Application to instationary flows on a stepped spillway." *International Journal of Multiphase Flow*, Vol. 58, January 2014, pp. 139-153, DOI: 10.1016/j.ijmultiphaseflow.2013.09.006.

Felder, S. and Chanson, H. (2014b). "Effects of step pool porosity upon flow aeration and energy dissipation on pooled stepped spillways." *Journal of Hydraulic Engineering*, Vol. 140, No. 4, pp. 04014002-1-04014002-11, DOI: 10.1061/(ASCE)HY.1943-7900.0000858.

Flow Science Inc. (2005). *FLOW-3D user's manual (version 9.0),* Flow Science Inc., Santa Fe, NM.

Frizell, K. and Melford, B. (1991). "Designing spillways to prevent cavitation damage." *Concrete International*, Vol. 13, No. 5, pp.58-64.

Frizell, K. H. (1991). "Stepped spillway design for flow over embankment." *Proc. Nat. Conf. Hydraulic Engineering,* ASCE, Vol. 2, Nashville, Tennessee, pp. 118-123.

Frizell, K. W., Renna, F. M., and Matos, J. (2013). "Cavitation potential of flow on stepped spillways." *Journal of Hydraulic Engineering*, Vol. 139, No. 6, pp. 630-636, DOI: 10.1061/(ASCE)HY.1943-7900.0000715.

Gang, L., Jian-min, Z., Jian-Gang, C., Fei, Y., and Lu, L. (2011). "3-D Numerical simulation research of flow in a vortex drop shaft which have two volute chambers with aeration." *Proceedings of the 34th World Congress of the International Association for Hydro-Environment Research and Engineering: 33rd Hydrology and Water Resources Symposium and 10th Conference on Hydraulics in Water Engineering* (p. 1779), Engineers Australia.

Gomes, J., Marques, M., and Matos, J. (2007). "Predicting cavitation inception on steeply sloping stepped spillways." *Proc., 32nd IAHR Congress, International Assoc. for Hydraulic Research*, Venice, Italy.

Khatsuria, R. M. (2004). *Hydraulics of spillways and energy dissipators*, CRC Press.

Khdhiri, H., Potier, O., and Leclerc, J. P. (2014). "Aeration efficiency over stepped cascades: Better predictions from flow regimes." *Water Research*, pp. 194-202.

Lobosco, R. J., H. E. Schulz, and A. L. A. Simões. (2011). "Analysis of two phase flows on stepped spillways." *Hydrodynamics - Optimizing Methods and Tools*.

Meireles, I., Renna, F., Matos, J., and Bombardelli, F. (2012). "Skimming, nonaerated flow on stepped spillways over roller compacted concrete dams." *Journal of Hydraulic Engineering*, Vol. 138, No. 10, pp. 870-877, DOI: 10.1061/(ASCE)HY.1943-7900.0000591.

Ohtsu, I., Yasuda, Y. (1997). "Characteristics of flow conditions of stepped channels." *Proc. 27th IAHR Congress, San Francisco, USA*, 583-588.

Peterka, A. J. (1953). "The effect of entrained air on cavitation pitting." *Proceedings Minnesota International Hydraulic Convention*, ASCE, 507-518.

Peterka, A. J. (1958). *Hydraulic design of stilling basins and energy dissipaters. engineering monograph*, No. 25, USBR, Denver, CO.

Peyras, L., Royet, P., and Degoutte, G. (1991). "Flows and dissipation of energy on gabion weirs." *J. Houille Blanche*, No. 1, pp. 37-47.

Pfister, M., Hager, W. H., and Minor, H. E. (2006). "Bottom aeration of stepped spillways." *Journal of Hydraulic Engineering*, Vol. 132, No. 8, pp. 850-853, DOI: 10.1061/(ASCE)0733-9429(2006)132:8(850).

Rajaratnam, N. (1990). "Skimming flow in stepped spillways." *Journal of Hydraulic Engineering*, Vol. 116, No. 4, pp. 587-591.

Rice, C. E. and Kadavy, K. C. (1996). "Model study of a roller compacted concrete stepped spillway." *Journal of Hydraulic Engineering*, Vol. 122, No. 6, pp. 292-297, DOI: 10.1061/(ASCE)0733-9429(1996)122:6(292).

Roushangar, K., Akhgar, S., Salmasi, F., and Shiri J. (2014). "Modeling energy dissipation over stepped spillways using machine learning approaches." *Journal of Hydrology*, Vol. 508, pp. 254-265, DOI: 10.1016/j.jhydrol.2013.10.053.

Rudman, M. (1997). "Volume-tracking methods for interfacial flow calculations." *International journal for numerical methods in fluids*, Vol. 24, No. 7, pp. 671-691, DOI: 10.1002/(SICI)1097-0363(19970415)24:7<671::AID-FLD508>3.0.CO;2-9.

Savage, B. M. and Johnson, M. C. (2001). "Flow over ogee spillway: Physical and numerical model case study." *Journal of Hydraulic Engineering*, Vol. 127, No. 8, pp. 640-649, DOI: 10.1061/(ASCE)0733-9429(2001)127:8(640).

Shahheydari, H. (2010). *Investigating on stepped spillway geometry to achieve maximum energy dissipation*, MSc Thesis, University of Sistan and Baluchestan, Zahedan, Iran.

Sorensen, R. M. (1985). "Stepped spillway hydraulic investigation." *Journal of Hydraulic Engineering*, Vol. 111, No. 12, pp. 1461-1472, DOI: 10.1061/(ASCE)0733-9429(1985)111:12(1461).

USBR (1977). *Design of small dams*, Bureau of Reclamation, Washington, D.C.

Vischer, D. L. and Hager, W. H. (1998). *Dam hydraulics*, Wiley & Sons, Chichester.

Wu, J. H., Zhang, B., and Ma, F. (2013). "Inception point of air entrainment over stepped spillways." *Journal of Hydrodynamics*, Ser. B, Vol. 25, No. 1, pp. 91-96, DOI: 10.1016/S1001-6058(13)60342-X.

Yakhot, V. and Smith, L. M. (1992). "The renormalization group, the -expansion and derivation of turbulence models." *Journal of Scientific Computing*, Vol. 7, No. 1, pp. 35-61.

Yakhot, V., Orszag, S. A., Thangam, S., Gatski, T. B. and Speziale, C. G. (1992), "Development of turbulence models for shear flows by a double expansion technique." *Physics of Fluids A: Fluid Dynamics (1989-1993),* Vol. 4, No. 7, pp. 1510-1520.

Zhang, J. M., Chen, J. G., Xu, W. L., and Peng, Y. (2013). "Characteristics of vortex structure in multi-horizontal submerged jets stilling basin." *Proceedings of the ICE - Water Management* (in press), DOI: 10.1680/wama.12.00071.

Zhang, J., Chen, J., and Wang, Y. (2012). "Experimental study on time-averaged pressures in stepped spillway." *Journal of Hydraulic Research*, Vol. 50, No. 2, pp. 236-240, DOI: 10.1080/00221686.2012.666879.

Zhao, C. H., Zhu, D. Z., Sun, S. K., and Liu, Z. P. (2006). "Experimental study of flow in a vortex drop shaft." *Journal of Hydraulic Engineering*, Vol. 132, No. 1, pp. 61-68, DOI: 10.1061/(ASCE)0733-9429(2006)132:1(61).